2017 21st International Conference on Process Control (PC)
June 6–9, 2017, Štrbské Pleso, Slovakia

Economic NMPC for Heat-Integrated Chemical Reactors

Julian Straus, Sigurd Skogestad
Department of Chemical Engineering
Norwegian University of Science and Technology
Trondheim, Norway
Email: {julian.straus, sigurd.skogestad}@ntnu.no

***Abstract*—This paper presents the application of economic NMPC for a heat-integrated chemical reactor. The chosen case study is given by the ammonia synthesis reactor. Through the application of economic NMPC, it is possible to move the operating point close to the unstable region, corresponding to a 12% increase in the extent of reaction with nominal operations conditions. As a further advantage, the increased conversion of ammonia corresponds to a higher outlet temperature of the system which can be utilized to produce high and medium pressure steam. The proposed economic NMPC is able to adjust in the case of disturbances fast to the new optimal conditions and maintains the productivity of the reactor without engaging into limit-cycle behaviour or extinction of the reactor**

I. INTRODUCTION

Heat-integrated chemical reactors are generally applied in the case of exothermic reactions to utilize the generated heat for preheating the inlet flow to the reaction temperature. Examples include the ammonia synthesis reactor [1] and the methanol synthesis [2]. In addition to heat-integration between the inlet and outlet of reactors, separation of the reactor into several smaller beds with quench flows and/or heat removal through heating up the feed can move the equilibrium temperature at the reactor outlet to favoured lower temperatures resulting in a higher conversion per reactor pass.

However, due to the reluctance of industry to use automated control for the split-ratios between different reactor beds and the recycle heat exchanger, limit cycle behaviour can occur in the case of disturbances like a pressure or temperature drop with potential extinction of the chemical reaction. In order to counteract this behaviour, operation points away from the optimal conditions have to be chosen to improve the stability of the reactor. Nonetheless, the system stability is not guaranteed for large disturbances. Morud and Skogestad [3] showed that this behaviour is caused by a combination of positive feedback by the preheater and an inverse response of the reactor outlet temperature to a step change in the reactor inlet temperature. For the same case study, Naess [4] proposed a controller based on the inlet temperature of the respective beds with an additional split range controller for controlling the ratio between the flow through the heat exchanger and quench flow 1. However, no dynamic simulation results showing the performance of this control structure were presented. As the optimal temperature can vary depending on the disturbance, economical NMPC can serve as an interesting alternative to the above mentioned control structure for controlling the split ratios and hence the reactor.

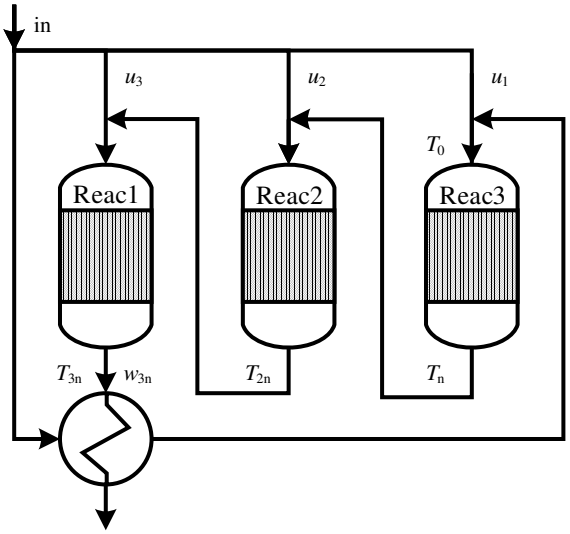

Fig. 1. Heat-integrated 3 bed reactor system of the ammonia synthesis gas loop.

II. MODEL AND PROCESS DESCRIPTION

A. Model assumptions

The process model is similar to the one used by Morud and Skogestad in their analysis of the limit-cycle behaviour [3]. The process itself consists of 3 sequential reactor beds and is shown in Fig. 1. The feed (denoted by $_{in}$) is split into 4 streams defined by 3 split-ratios which correspond to the manipulated variables $\mathbf{u} = [u_1 \ u_2 \ u_3]^\mathsf{T}$. In addition for preheating the feed to the first reactor bed, one of the streams is heated through the reactor effluent in a heat exchanger to increase the inlet temperature of the first bed. This results into the above mentioned positive feedback. In order to simplify the mathematical model, the following assumptions are made:

- there is no pressure drop in the system;
- the heat capacity of the streams are independent of composition and temperature;
- there is a perfect low level ratio controller controlling the split ratios;

TABLE I
NOMENCLATURE OF THE STATES AND DECISION VARIABLES.

State	Description	Lower bound	Upper bound
x	Temperatures **T** [°C]	200	600
z	Mass fractions NH_3 **w** [wt%]	0	100
u	Split ratios **u** [%]	0	100

- the change in the split ratios can be assumed to be instantaneous, and hence, dynamics for the valves do not need to be incorporated;
- the reactor beds can be modelled as continuously stirred tank reactor (CSTR) cascade. This corresponds to a discretization of the partial differential equation of a plug-flow reactor along the x-axis;
- there is a time-scale separation between the changes in the concentration and the temperature. Hence, it is possible to assume that the concentration is at steady-state in the investigated reactor section.
- the gas hold-up in the sections of the bed is assumed to be constant;
- the mixing of the streams before the reactor beds is perfect;
- the heat capacity of the process gas is negligible compared to heat capacity of the catalyst bed;

Based on the above mentioned assumptions, a differential algebraic formulation is proposed in the following sections. The differential equations represent the temperature evolution within the sections of each reactor bed whereas the algebraic equations define the concentrations within the sections of the reactor beds. The definition of the states and parameters are given in the Tables I and II.

B. Reactor model

The reaction rate as a function of the partial pressure $p_{i,j}$ in the CSTR reactor j of the cascade is given by the Temkin-Pyzhev equation as described by Froment [5].

$$r_{N_2,j} = k_{j,1}\frac{p_{N_2,j}p_{H_2,j}^{\frac{3}{2}}}{p_{NH_3,j}} - k_{j,-1}\frac{p_{NH_3,j}}{p_{H_2,j}^{\frac{3}{2}}} \tag{1}$$

in which the reaction constants $k_{j,\pm1}$ are given by the Arrhenius equation:

$$k_{j,\pm1} = A_{0,\pm1}e^{-\frac{E_{a,\pm1}}{R(T_j+273.15)}} \tag{2}$$

This reaction rate is written in [kmol N_2/ m^3_{cat} h] and hence, the reaction rate in [kg NH_3/kg_{cat} h] needed for the mass and temperature balances is then given by

$$r_{NH_3,j} = f r_{N_2,j}\frac{2\times 17}{\rho_{cat}} \tag{3}$$

The reaction rate is multiplied with a factor of $f = 4.75$ to match plant data as explained by Morud and Skogestad [3]. The change in the temperature in each subsection of the reactor is then given by

$$\frac{dT_j}{dt} = \frac{c_{p,gas}\left(\dot{m}_{j-1}T_{j-1} - \dot{m}_j T_j\right) + m_{cat,j}r_{NH_3,j}\Delta H_{rx}}{m_{cat,j}c_{p,cat}} \tag{4}$$

TABLE II
NOMENCLATURE OF PARAMETERS AND CALCULATED VALUES.

Variable	Description	Value	Unit
$A_{0,+1}$	Arrhenius factor, forward	1.79×10^4	-
$A_{0,-1}$	Arrhenius factor, backward	2.57×10^{16}	-
$E_{a,+1}$	Activation Energy, forward	87,090	J/mol
$E_{a,-1}$	Activation Energy, backward	198,464	J/mol
R	Universal gas constant	8.314	J/mol/K
ρ_{cat}	Catalyst density	2,200	kg/m^3
$c_{p,gas}$	Gas heat capacity	3,500	J/kg/K
$c_{p,cat}$	Catalyst heat capacity	1,100	J/kg/K
$m_{cat,R1}$	Catalyst mass bed 1	14,718	kg
$m_{cat,R2}$	Catalyst mass bed 2	21,186	kg
$m_{cat,R3}$	Catalyst mass bed 3	33,440	kg
$m_{cat,j}$	Catalyst mass in volume j	depending	kg
$\dot{m}_j$	Mass flow in volume j	depending	kg/s
ΔH_{rx}	Heat of reaction	-2.7×10^6	J/kg NH_3
U	Heat transfer coefficient	536	W/m^2/K
A	Heat exchanger area	283	m^2

whereas the component balances can be written as

$$0 = \dot{m}_{j-1}w_{j-1} - \dot{m}_j w_j + r_{NH_3,j}m_{cat,j} \tag{5}$$

C. Heat exchanger model

The heat exchanger is modelled using the number of transfer units (NTU) method. In this method, the NTU and the ratio of the enthalpy (C^*) of the cold (subscript c, feed) and hot stream (subscript h, outlet bed 3) are calculated and based on these values, the effectiveness (ε) can be calculated in Eq. (8).

$$C^* = \frac{\dot{m}_c c_{p,gas}}{\dot{m}_h c_{p,gas}} \tag{6}$$

$$NTU = \frac{UA}{\dot{m}_c c_p} \tag{7}$$

$$\varepsilon = \frac{1-e^{-NTU(1-C^*)}}{1-C^*e^{-NTU(1-C^*)}} \tag{8}$$

This effectiveness corresponds to the percentage of the maximum achievable energy transfer Q as shown in Eq (9).

$$\begin{aligned} Q &= \varepsilon Q_{max} \\ &= \varepsilon\dot{m}_c c_{p,gas}(T_{in,h} - T_{in,c}) \end{aligned} \tag{9}$$

Due to the assumption of a constant heat capacity, the outlet temperatures of the heat exchanger are then given as

$$T_{out,h} = T_{in,h} - \frac{Q}{\dot{m}_h c_{p,gas}} \tag{10}$$

$$T_{out,c} = T_{in,c} + \frac{Q}{\dot{m}_c c_{p,gas}} \tag{11}$$

It has to be noted, that these model equations do not add a further differential of algebraic equation to the system. This is caused by the fact, that the equations define a relationship between the temperature of the first CSTR in the first bed and the outlet temperature of the last bed. As the inlet temperature of a bed is not a state, no additional algebraic equations are defined.

D. Stream mixing and general requirement

The equations of mixing two streams 1 and 2 for the temperature and concentrations are given as

$$T_{mix} = \frac{\dot{m}_1}{\dot{m}_1 + \dot{m}_2} T_1 + \frac{\dot{m}_2}{\dot{m}_1 + \dot{m}_2} T_2 \tag{12}$$

$$w_{mix} = \frac{\dot{m}_1}{\dot{m}_1 + \dot{m}_2} w_1 + \frac{\dot{m}_2}{\dot{m}_1 + \dot{m}_2} w_2 \tag{13}$$

Similar to the heat exchanger equations, they do not increase the number of algebraic equations as they are purely defining relationships between the outlet states of the previous bed and the inlet of the following bed. The inlet temperature of bed 1 is in the following denoted as T_0 as it has an important influence on the occurrence of limit-cycle behaviour.

Due to mass conservation, the following inequality constraint for the decision variables $\mathbf{u}$ has to be fulfilled as well.

$$h(\mathbf{u}) = \sum_i u_i - 1 \leq 0 \tag{14}$$

E. Optimization of the system

The differential states are defined as the temperatures $\mathbf{x} = \mathbf{T}$, the algebraic states as the weight fractions $\mathbf{z} = \mathbf{w}$. Both type of states have a total of $3n$ input variables per time step in which n defines the number of discrete volumes in each of the 3 reactors (*vide supra*). The manipulated variables are 3 per time step and correspond to the split ratio to the inlets of the reactor beds. To summarize, we can write

$$\mathbf{x} \in \mathbb{R}^{3n} \tag{15}$$

$$\mathbf{z} \in \mathbb{R}^{3n} \tag{16}$$

$$\mathbf{u} \in \mathbb{R}^{3} \tag{17}$$

The corresponding non-linear problem constraints are given in semi-explicit representation by

$$\begin{aligned} \dot{\mathbf{x}} &= \mathbf{F}(\mathbf{x}, \mathbf{z}, \mathbf{u}) \\ 0 &= \mathbf{G}(\mathbf{x}, \mathbf{z}, \mathbf{u}) \\ 0 &\geq h(\mathbf{u}) \end{aligned} \tag{18}$$

in which $\mathbf{F}$ corresponds to the differential equations of the temperature defined in Eq. (4), $\mathbf{G}$ to the algebraic equations defined in Eq. (5), and $h(\mathbf{u})$ to the input inequality defined in Eq. (14). Furthermore, bounds on the variables are defined in Table I. This system represents an index 1 differential algebraic system which can be verified by taking the total differential of $\mathbf{G}(\mathbf{x}, \mathbf{z}, \mathbf{u})$ given by

$$\frac{\mathrm{d}}{\mathrm{d}t}\mathbf{G}(\mathbf{x}, \mathbf{z}, \mathbf{u}) = \frac{\partial \mathbf{G}}{\partial \mathbf{x}}\mathbf{F} + \frac{\partial \mathbf{G}}{\partial \mathbf{z}}\dot{\mathbf{z}} + \frac{\partial \mathbf{G}}{\partial \mathbf{u}}\dot{\mathbf{u}} = 0 \tag{19}$$

The optimisation was performed using CasADi [6] with IPOPT [7]. The optimal control problem (OCP) was solved *via* the direct collocation method [8] with RADAU order 3 as collocation points. The used integrator for the simulation is IDAS, which is part of the SUNDIALS package [9], with a fixed integrator step length of t_{int}.

III. OPTIMAL CONTROL PROBLEM FORMULATION

As mentioned in the introduction, the split-ratios in-between the beds of an ammonia plant are chosen to avoid limit-cycle behaviour. However, these split-ratios are suboptimal with respect to the conversion within the reactor. Hence, steady-state optimization for finding the optimal split-ratio is conducted.

A. Problem statement

The constraints for the steady-state system are defined by Eq. (18) with $\dot{\mathbf{x}} = 0$. The number of discrete volumes in each reactor bed is chosen to be $n = 10$ as in this case, the actual diffusion is cancelled by "numerical" diffusion [3]. This results in a non-linear problem with 30 algebraic and 30 dynamic states ($n = 10$) as well as 3 decision variables. The aim is to maximize the extent of reaction of ammonia which is defined as

$$\xi = \dot{m}_{in}\,(w_{30} - w_{in}) \quad \text{in [kg NH}_3\text{/ s]} \tag{20}$$

The sole maximization of the extent of reaction furthermore reduces the cost in the separation and synthesis gas make-up section through a reduction of the recycle stream and hence reduced compressor power in the recycle compressor. A higher extent of reaction additionally increases the outlet temperature of the system, which can be utilized to produce high-pressure stream for the reformer as this process requires a large amount of energy due to its endothermic nature. For a given feed, this can be simplified to the following non-linear problem

$$\begin{aligned} \min_{\mathbf{x},\mathbf{z},\mathbf{u}} \quad & -w_{30} \\ \text{s.t.} \quad & 0 = \mathbf{F}(\mathbf{x}, \mathbf{z}, \mathbf{u}) \\ & 0 = \mathbf{G}(\mathbf{x}, \mathbf{z}, \mathbf{u}) \\ & 0 \geq h(\mathbf{u}) \end{aligned} \tag{21}$$

B. Results

The results of the steady-state optimization are given in Table III. As only the produced ammonia is interesting (*vide supra*), the extent of reaction as defined in Eq. (20) is used. The change in produced ammonia corresponds to a 12% increase compared to the nominal case. Especially the split ratios to reactor beds 2 and 3 were increased, as this indicates a reduction in temperature at the inlet of the respective bed which results in a lower equilibrium temperature at the reactor outlet and hence higher conversion. The temperature and concentration profiles of the optimized system as well as the original system are given in Figure 2.

TABLE III
RESULTS OF THE STEADY-STATE OPTIMIZATION.

	Split ratio reactor 1	Split ratio reactor 2	Split ratio reactor 3	ξ [kg NH_3/ s]
Nominal	0.2302	0.1389	0.1270	16.2147
Optimal	0.2124	0.3079	0.2958	18.1797

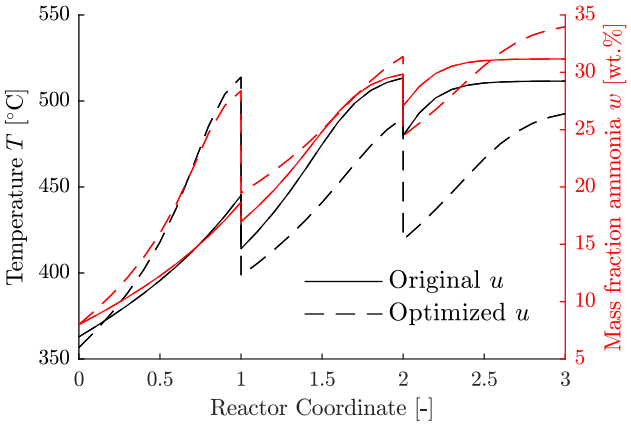

Fig. 2. Reactor profile for the optimized and nominal operation conditions ($\dot{m}_{in} = 70$ kg/s, $p_{in} = 200$ bar, $T_{in} = 200$ °C, and $w_{in} = 8$ wt%) and steady state.

C. Discussion

The steady-state optimization improves the reactor utilization in the system. This is directly visible in Figure 2 as with the nominal split-ratios, half of reactor bed 3 is not utilized. This is indicated by the flat temperature and concentration profiles at the end of the reactor in the nominal case. A further improvement is given by the larger residence time in the first two reactor beds. However, the problem in this reactor system is the occurrence of limit-cycle behaviour or reactor extinction (*vide supra*), and hence, dynamic simulations with disturbances were conducted to compare the performance. Figure 3 shows a pressure disturbance of $\Delta p_{in} = -20$ bar occurring after $t = 10$ min and the return to nominal conditions at $t = 75$ min. The same discretization as in the case of the nominal solution was used. Due to the changed residence time, this is not entirely correct to counteract the actual diffusion, but can be utilized nevertheless as the migration velocity for the temperature wave is even lower in the optimized case resulting in even faster reactor extinction.

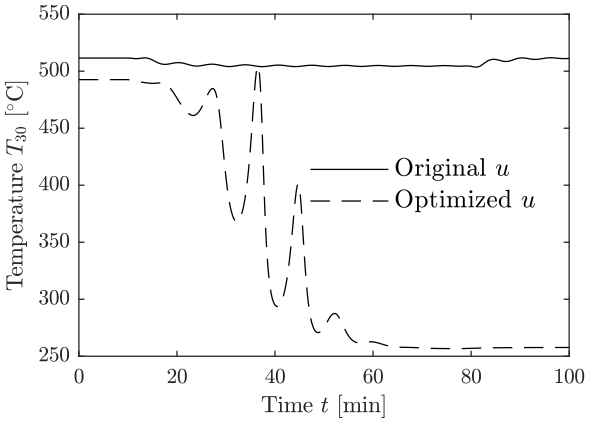

Fig. 3. Outlet temperature of Bed 3 with a pressure drop of $\Delta p_{in} = -20$ bar at $t = 10$ min and back to nominal conditions at $t = 75$ min with a constant input u corresponding to manual operation (open loop).

As we can see, the optimized split-ratios decrease the potential of the system to reject disturbances. Hence, automated control is necessary and the application of NMPC will be discussed in the following section.

IV. Non-Linear Model Predictive Control Formulation

As shown in the section of the steady state optimization, it is necessary to have automated control if the optimal operation point should be implemented. This can be decentralized feedback control as proposed by Morud and Skogestad [3] or economic NMPC. Alternatively, it is also possible to apply real-time-optimization with set-point tracking NMPC. However, set-point tracking NMPC is difficult to implement for this system as, depending on the disturbance, defined set-points may not be reached. Hence, the economic NMPC approach is chosen in this paper.

A. Problem statement

The constraints of the NMPC are given by Eq. (18). Additional to the cost function of the steady state problem in Eq. (21) a penalty term for input usage is introduced. This results in the following cost function at each step of the moving horizon

$$J_{dyn} = -w_{30} + \dot{\mathbf{u}}^{\top}\mathbf{R}\dot{\mathbf{u}} \tag{22}$$

This corresponds to an optimal control problem given by

$$\begin{aligned} \min_{\mathbf{x}(\cdot),\mathbf{z}(\cdot),\mathbf{u}(\cdot)} \quad & \int_0^{t_{max}} -w_{30} + \dot{\mathbf{u}}^{\top}\mathbf{R}\dot{\mathbf{u}}\; dt \\ \text{s.t.} \quad & \dot{\mathbf{x}} = \mathbf{F}(\mathbf{x},\mathbf{z},\mathbf{u},t), && t \in [0, t_{max}] \\ & 0 = \mathbf{G}(\mathbf{x},\mathbf{z},\mathbf{u},t), && t \in [0, t_{max}] \\ & 0 \geq h(\mathbf{u},t), && t \in [0, t_{max}] \end{aligned} \tag{23}$$

The parameters shown in Table IV are used as tuning parameters of the NMPC. Morud shows [3], that the time the temperature wave requires to move through the reactor is given by roughly 350 s. Hence, it is necessary, that the NMPC horizon is at least 350 s long to capture this. Due to the change in the input variables, the residence time in the first two reactors is increased and hence, the interval should be even longer. As the interval in the beginning of the NMPC should be accurate, input blocking is applied using an increasing block length for the input of $\begin{bmatrix}1 & 1 & 1 & 2 & 2 & 2 & 5 & 6\end{bmatrix} t_{block,NMPC}$ in which the input is not changed. This corresponds to a total time frame of 600 s. The $\mathbf{R}$ was chosen to limit the input

TABLE IV
Tuning parameters for the NMPC optimization.

Parameter	Value	Unit
Integrator step length t_{int}	1	s
Input movement penalty $\mathbf{R}$	$\text{diag}(\begin{bmatrix}20 & 20 & 20\end{bmatrix})$	-
Sampling time $t_{samp,NMPC}$	30	s
Block time $t_{block,NMPC}$	30	s
Horizon	20	-

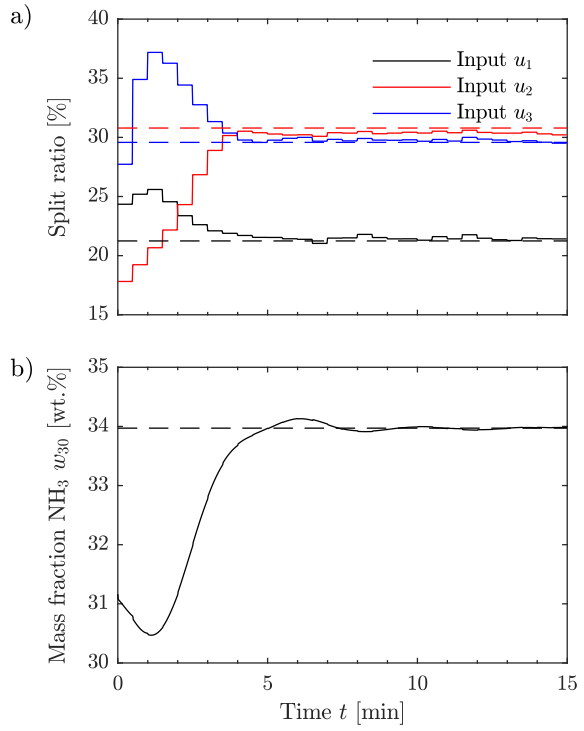

Fig. 4. Response of the split ratios a) and the ammonia mass fraction b) during startup of the NMPC at nominal conditions ($\dot{m}_{in} = 70$ kg/s, $p_{in} = 200$ bar, $T_{in} = 200$ °C, and $w_{in} = 8$ wt.%)

movement and avoid oscillatory behaviour while maintaining fast settlement to the new set-point.

Full state knowledge is assumed to simplify the calculations. Furthermore, it is assumed that the NMPC calculation is instantaneous. The investigated disturbances are input disturbances and assumed to have a measurement error given by Gaussian white noise with a standard deviation of $\sigma = 0.5\%$.

B. Results

During the start-up of the plant, economic NMPC is generally turned off as the model is fitted in the operation range as well as additional equipment like heaters may be used. Hence, the start-up of NMPC from nominal conditions was investigated in a first step to evaluate the possibility of switching from manual to automatic control. The results are plotted in Figure 4. The dashed lines in the following figures correspond to the optimal value for the given input conditions obtained in the steady state analysis. We can directly see an inverse response of the outlet mass fraction of ammonia. The economic NMPC controller is able to reach the optimal setpoint within five minutes and settles within the first ten minutes to the optimal value given in Table III. Small oscillations around the optimal concentration are hereby caused by the Gaussian white noise.

To evaluate the performance of the control structure on disturbance rejection, simulations with disturbance changes in all inlet conditions were conducted. Here, one-directed disturbances are applied as disturbances in the other direction may

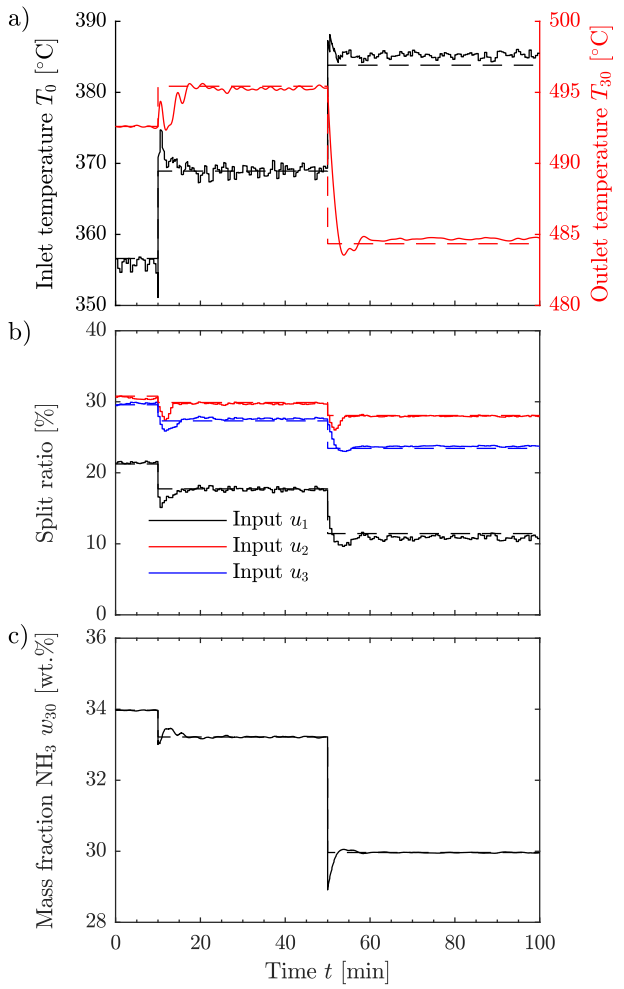

Fig. 5. Response of the inlet (T_0) and outlet (T_{30}) temperature a), the split ratios u_i b), and the ammonia mass fraction at the outlet w_{30} with start at nominal conditions and as disturbance an inlet flowrate increase of $\Delta\dot{m}_{in} = 15$ kg/s at $t = 10$ min and back to nominal flow rate at $t = 50$ min with a simultaneous pressure drop of $\Delta p_{in} = -50$ bar.

lead to sub-optimal behaviour, but no limit-cycle behaviour or reactor extinction as the extent of reaction is increased in this case increasing the outlet temperature of reactor bed 3, T_{30} and hence increasing the inlet temperature of bed 1, T_0.

Disturbances in the inlet flowrate $\dot{m}_{in}$ as well as the pressure of the system p_{in} are presented in Figure 5. This flowrate change increase and pressure drop is generally quite large. Flowrate increases can occur during the operation if problems with the purge control are present. They can lead to reactor extinction due to reduced residence time and hence reduced extent of reaction. Similarly, pressure drops can occur if problems with the compressor trains exists and result in the same problem as in the case of an increased inlet flowrate due to a reduction in the reaction rate and of the equilibrium concentration. As shown in Figure 3, already a pressure drop of $\Delta p_{in} = -20$ bar lead to unstable performance in manual mode using the optimized input values without adjustment.

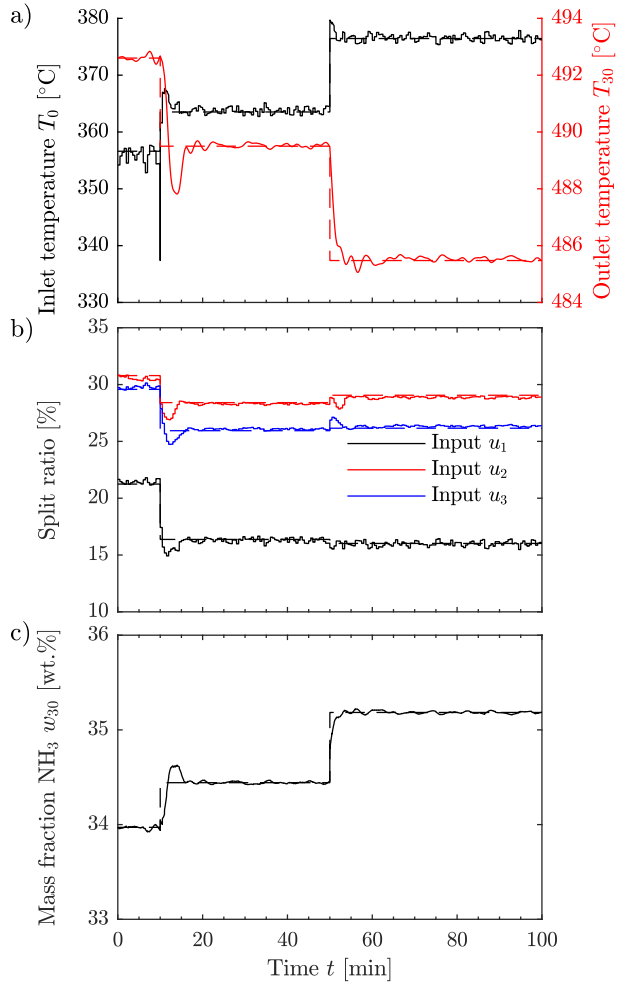

Fig. 6. Response of the inlet (T_0) and outlet (T_{30}) temperature a), the split ratios u_i b), and the ammonia mass fraction at the outlet w_{30} with start at nominal conditions and as disturbance a temperature drop of $\Delta T_{in} = -30$ °C at $t = 10$ min and back to nominal inlet temperature at $t = 50$ min with a simultaneous concentration increase of $\Delta w_{in} = 4$ wt.%.

The application of economic NMPC however give in the case of both disturbances close to optimal behaviour. The settling time of the optimized outlet mass fraction of ammonia corresponds to about 10 min as it was already the case in the startup of the NMPC.

Disturbances in the inlet temperature T_{in} as well as the inlet mass fraction w_{in} are presented in Figure 6. Temperature reduction in the inlet can be present if the preheating control is faulty and can result in a lower inlet temperature of the first bed. Concentration increases on the other hand can occur of the ammonia separation temperature is too high and the ammonia concentration in the recycle increases. Similarly to the pressure and flowrate disturbance, the temperature drop and ammonia mass fraction increase can be handled by the economic NMPC. Again, the settling time to the nominal optimum is around 10 min. The inlet temperature of the first bed is increasing for all disturbances showing the reduced extent of reaction in the beds and hence reduced heat of reaction. Additionally, the variation in the outlet temperature is way smaller than the variation in the inlet temperature due to the equilibrium.

C. Discussion

The rejection of all disturbances which would lead in the case of manual operations to limit-cycle behaviour or extinction of the reactor shows the performance of the chosen controller configuration. It is interesting to note that for all disturbances, the quench flows are reduced compared to the nominal case. This reduction increases the preheating of the feed to the first bed and increases the above mentioned inlet temperature.

The assumption of full state feedback is generally not possible to achieve in practice where state estimators have to be used. Temperature measurements can be implemented at least at the inlet and outlet of each bed. As the median of the optimization time is around 2.5 s and the maximum 6 s on an Intel® Core™ i5-6600K, the assumption of instantaneous calculations can be seen valid with a sampling time of $t_{NMPC} = 30$ s.

V. CONCLUSIONS AND OUTLOOK

An economic non-linear model predictive controller was introduced for the control of the split ratios in an ammonia synthesis reactor.The application of the controller yields the optimal conversion of ammonia in the case of input disturbances. The tuning of this controller was performed by trial-and-error, and hence, potential improvements of the performance of the controller are possible.

Further work could include the implementation of the new step obtained via NMPC only after the time in the integrator is passed the solution time needed. This would give a more realistic view on the performance of the controller.

REFERENCES

[1] M. Appl, *Ammonia, 2. Production Processes*. Wiley-VCH Verlag GmbH & Co. KGaA, 2000.

[2] D. Santangelo, V. Ahn, and A. Costa, "Optimization of methanol synthesis loops with quench reactors," *Chemical Engineering & Technology*, vol. 31, no. 12, pp. 1767–1774, 2008.

[3] J. C. Morud and S. Skogestad, "Analysis of instability in an industrial ammonia reactor," *AIChE Journal*, vol. 44, no. 4, pp. 888–895, 1998.

[4] L. Naess, A. Mjaavatten, and J.-O. Li, "Using dynamic process simulation from conception to normal operation of process plants," *Computers & Chemical Engineering*, vol. 17, no. 5, pp. 585 – 600, 1993.

[5] G. Froment, K. Bischoff, and J. De Wilde, *Chemical Reactor Analysis and Design, 3rd Edition*. John Wiley & Sons, Incorporated, 2010.

[6] J. Andersson, "A General-Purpose Software Framework for Dynamic Optimization," PhD thesis, Arenberg Doctoral School, KU Leuven, Department of Electrical Engineering (ESAT/SCD) and Optimization in Engineering Center, Kasteelpark Arenberg 10, 3001-Heverlee, Belgium, October 2013.

[7] A. Wächter and L. T. Biegler, "On the implementation of an interior-point filter line-search algorithm for large-scale nonlinear programming," *Mathematical Programming*, vol. 106, no. 1, pp. 25–57, 2006.

[8] L. T. Biegler, *10. Simultaneous Methods for Dynamic Optimization*, pp. 287–324.

[9] A. C. Hindmarsh, P. N. Brown, K. E. Grant, S. L. Lee, R. Serban, D. E. Shumaker, and C. S. Woodward, "SUNDIALS: Suite of nonlinear and differential/algebraic equation solvers," *ACM Transactions on Mathematical Software (TOMS)*, vol. 31, no. 3, pp. 363–396, 2005.